

Negative refraction in nonlinear wave systems

Zhoujian Cao¹, Hong Zhang², and Gang Hu^{1*}

¹*Department of physics, Beijing Normal University, Beijing, 100875, China and*

²*Zhejiang Institute of Modern Physics and Department of Physics, Zhejiang University, Hangzhou 310027, China*

(Dated: April 24, 2018)

Abstract

People have been familiar with the phenomenon of wave refraction for several centuries. Recently, a novel type of refraction, i.e., negative refraction, where both incident and refractory lines locate on the same side of the normal line, has been predicted and realized in the context of linear optics in the presence of both right- and left-handed materials. In this work, we reveal, by theoretical prediction and numerical verification, negative refraction in nonlinear oscillatory systems. We demonstrate that unlike what happens in linear optics, negative refraction of nonlinear waves does not depend on the presence of the special left-handed material, but depends on suitable physical condition. Namely, this phenomenon can be observed in wide range of oscillatory media under the Hopf bifurcation condition. The complex Ginzburg-Landau equation and a chemical reaction-diffusion model are used to demonstrate the feasibility of this nonlinear negative refraction behavior in practice.

PACS numbers: 82.40.Ck, 05.45.-a, 47.54.+r, 89.75.Kd

* Author for correspondence: ganghu@bnu.edu.cn

It is well known that light can refract at interface of two media. For several centuries only positive refraction has been found in nature, where incident line and refractory line locate on either side of the normal line of the interface. Very recently, a new type of optical refraction—negative refraction, where both incident and refractory lines locate on the same side of the normal line of the interface, has been theoretically predicted [1] and experimentally observed [2] when refraction occurs between a right-handed material and a left-handed material where optical waves propagate inward to the wave source. In addition, some new observations have been reported in nonlinear wave propagation, and one particularly interesting phenomenon is antispiral waves [3, 4, 5, 6, 7, 8]. In contrast to spirals (which are familiar to people) where waves propagate outwards from the tips, antispiral waves propagate inward to the spiral tip, the wave source. Because the existence of inwardly propagating waves is key to generate negative refraction in linear optics, we expect that the novel phenomenon of negative refraction may also be observed in other nonlinear wave systems where antispirals and inwardly propagating waves can be found.

In this letter, we go further from the above phenomena of negative refraction in linear optics and antispirals in nonlinear waves propagation by revealing a new type of negative refraction in nonlinear oscillatory systems. We demonstrate that unlike what happens in linear optics, negative refraction of nonlinear waves does not require special left-handed materials, rather, it can be found in wide range of media under suitable nonlinear condition of Hopf bifurcation. To demonstrate this new phenomenon, we use the complex Ginzburg-Landau equation (CGLE) as our example. With this model, we are able to freely generate, by periodic forcing, both normal waves (NWs) and antiwaves (AWs), of which NWs propagate outward from the wave source while AWs propagate towards the wave source. An interesting feature of negative refraction is observed when waves on either side of the interface have different propagation characteristics, one AW and the other NW. Moreover, we use a typical chemical reaction diffusion model, the Brusselator, to verify the prediction of negative refraction of CGLE. This suggests possible experimental realization of negative refraction in nonlinear chemical reaction diffusion systems.

We consider 2D CGLE with local periodic forcing [9]

$$\frac{\partial A}{\partial t} = A - (1 + i\alpha)|A|^2A + (1 + i\beta)\nabla^2A + \delta(x)Fe^{-i\omega_{in}t} \quad (1)$$

where no-flux (Neumann) condition is applied to all boundaries. The last term on the right

side of the equation, an additive periodic forcing with constant amplitude F , serves as a wave source applied to the $x = 0$ stripe of the medium. F needs to be sufficiently large so that periodic waves can be stimulated, which will then propagate as planar waves into the unforced region of $x > 0$. We use $F = 1$ throughout this paper. The forcing frequency ω_{in} has its sign, which denotes the rotating direction of the forcing in the complex plane, “+” clockwise and “-” anticlockwise. In the absence of the source term ($F = 0$), Eq.(1) describes the onset of homogeneous oscillation through Hopf bifurcation, and this equation is used extensively as a typical model for describing rich behaviors of spatiotemporal chaos, propagating waves and pattern formations [10, 11, 12, 13, 14, 15].

In Fig.1, we fix $\beta = -1.4$ and demonstrate distinctive dynamical behaviors of the systems for different α and ω_{in} . Some parameter combinations generate NW (Fig. 1(a)), while others generate AW (Fig. 1(b)). The parameter regions in Fig. 1(c) indicated by NW and AW show NW and AW outputs, respectively, with $\omega = \omega_{in}$ (ω denotes the output frequency). In the shadowed region, the periodic forcing cannot control the system, and thus the system motion under periodic forcing is either periodic with $\omega \neq \omega_{in}$, or chaotic with broad band frequency spectrum. In this study we are not interested in the shadowed region, and will focus on the NW and AW regions only where $\omega = \omega_{in}$. Interestingly, all the NW and AW regions locate in the vicinity of the diagonal line $\omega = \omega_{in} = \alpha$. Since α is the bulk oscillation frequency ($\omega_o = \alpha$) of the local dynamics, all the NW and AW regions of Fig.1(c) satisfy resonance condition ($\omega_{in} \approx \omega_o = \alpha$). Moreover, in Fig. 1(c) it is clear that AWs appear only under the condition

$$\omega\omega_0 > 0 \text{ and } |\omega| < |\omega_0| = |\alpha| \quad (2)$$

NWs can be observed under the conditions of $\omega\omega_0 < 0$ or $|\omega| > |\omega_0|$ for $\omega\omega_0 > 0$. The boundaries between the parameter domains of NW and AW can be determined by the sign change of the phase velocity [7] $v_{phase} = \frac{\omega}{k}$. The transitions between NW and AW thus occur at two boundaries: $\omega = 0$ and $k = 0$. The former boundary justifies the transition between AW and NW with stationary Turing patterns $\omega = \omega_{in} = 0$ at the transition, and the latter defines the transition between AW and NW with homogeneous oscillation ($k = 0$) at the transition, which shrinks to a single point of $\alpha = \beta = \omega_{in}$ in Fig.1(c). In summary, we find that, with local forcing method, we can generate NWs and AWs freely. For instance, given an oscillatory medium with fixed parameters, we can produce both NW and AW by

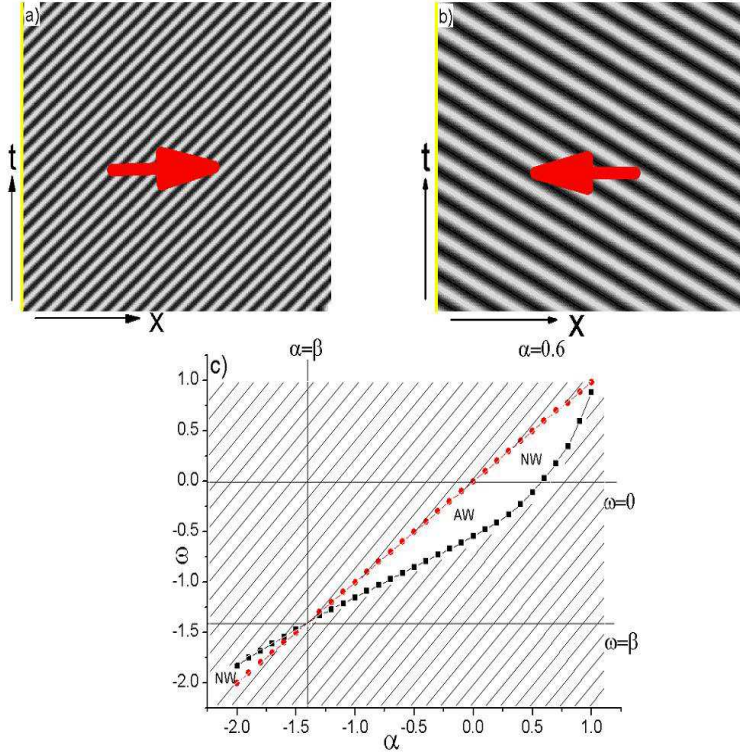


FIG. 1: In this and all the following figures, we apply no-flux (Neumann) boundary condition. $\beta = -1.4$, $F = 1.0$ are used in Figs.1 and 3 and 256×256 rectangular geometry is used for numerical simulations in Fig.1. (a & b) Numerical results of spatiotemporal patterns at $y = 128$, $x \in [0, 256]$ with different periodic forces applied on the left boundary of the rectangular system. Arrows denote the wave propagation directions. Space discretization of 256×256 pixels and time step $\Delta t = 0.05$ are used for numerical simulations. (a): Normal forward propagating waves (NWs). $\alpha = 0.2$, $\omega = \omega_{in} = -0.15$. (b): Planar antiwaves whose phase propagates toward the wave source. $\alpha = 0.2$, $\omega = \omega_{in} = 0.15$. (c): Distributions of different characteristic regions in $\omega_{in} - \alpha$ plane. Shaded region: no stable waves with $\omega = \omega_{in}$ can be realized in Eq.(1) whatever the input frequency ω_{in} . NW white region: normal waves of $\omega = \omega_{in}$ can be observed; AW white region: antiwaves of $\omega = \omega_{in}$ can be observed.

changing the forcing frequency ω_{in} only. This is different from antispirals in autonomous systems which produce either NW or AW (not both) with a single spiral frequency selected at the given set of parameters.

Now we come to the problem of nonlinear wave refraction. We consider planar waves passing an interface of two media with different parameters α , β (Fig. 2). Analogous to

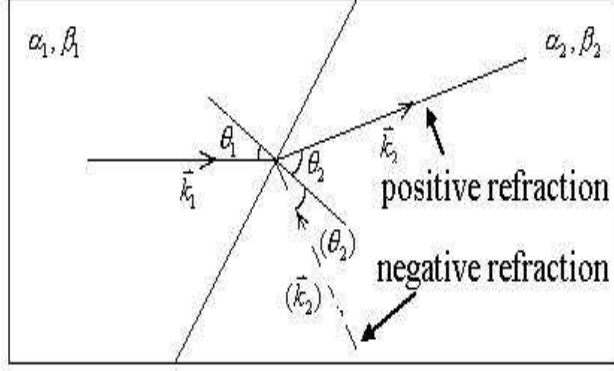


FIG. 2: Schematic figure of nonlinear refraction. The left and right regions are CGLE systems with parameters α_1, β_1 and α_2, β_2 , respectively. The middle line from left below to right up is the interface. The line marked with $\vec{k}_1, \vec{k}_2, (\vec{k}_2)$ are incident line, positive refractory line, and negative refractory line, respectively.

optics, the incident line and refractory line are perpendicular to the wave fronts in the two media. The incident angle (θ_1) is defined as the angle between the normal line and the incident line, which is positive definite. The refractory angle (θ_2) is defined as the angle between the normal line and the refractory line, which is positive if the refractory and incident lines locate on either side of the normal line, and is negative otherwise.

In linear optics, the light refraction relation can be precisely computed, based on the continuity conditions at the interface. For nonlinear systems, there is no general theory to describe the law of nonlinear wave refraction although the continuity conditions are still valid at the interface. The difficulty is that no analytical solutions can be obtained around the interface of two nonlinear media. We approximate the solutions of Eq.(1) as planar wave solutions [16]

$$A_{1,2} = \sqrt{1 - k_{1,2}^2} e^{i(-\omega_{1,2}t + \vec{k}_{1,2} \cdot \vec{r})} \quad (3a)$$

$$\omega_{1,2} = \alpha_{1,2} + (\beta_{1,2} - \alpha_{1,2})k_{1,2}^2 \quad (3b)$$

in the left and right regions of Fig.2, respectively. The actual solutions around the interface certainly deviate from these planar wave solutions. For instance, the amplitude of $|A_1|$ and $|A_2|$ must change considerably in the interface region for satisfying the continuity conditions. Our assumption is that the interface causes only very weak influence to the phase distributions of the planar waves (this assumption is fully confirmed by our numerical simulations).

This assumption allows us to predict the nonlinear wave refraction law by applying the phase continuity hypothesis of the planar wave solutions on the interface:

$$-\omega_1 t + \vec{k}_1 \cdot \vec{r} = -\omega_2 t + \vec{k}_2 \cdot \vec{r} \quad (4)$$

Here, we consider the case of $\omega_1 = \omega_2$ only, otherwise the refractory pattern cannot be stationary [17]. Therefore, we have $\vec{k}_1 \cdot \vec{r} = \vec{k}_2 \cdot \vec{r}$ which leads to $k_1 \sin \theta_1 = k_2 \sin \theta_2$.

There are several interesting conclusions we can draw from Eq.(4). First, with the sign of ω fixed (e.g., positive ω) k_1 and k_2 can be positive (NW) or negative (AW). It tells us that if k_1 and k_2 have the same sign positive refraction will be observed. If k_1 and k_2 have different signs, i.e., from NW at left to AW at right or vice versa, nonlinear negative refraction, an analog of propagation of light from right- to left-handed material (or vice versa), emerges. Second, with the help of dispersion relation, we can define from Eq.(3b) an effective refractory index similar to that in optics as

$$n(\omega) = \pm \frac{1}{|\omega|} \sqrt{\frac{\omega - \alpha}{\beta - \alpha}} \quad (5)$$

where “+” for NW ($\omega\omega_0 < 0$ or $|\omega| > |\omega_0| = |\alpha|$ and $\omega\omega_0 > 0$) and “-” for AW ($\omega\omega_0 > 0$ and $|\omega| < |\omega_0|$). The generalized refraction law for nonlinear waves in CGLE can be expressed as

$$\frac{\sin \theta_1}{\sin \theta_2} = \frac{n_2}{n_1} \quad (6)$$

In the following, we conduct numerical simulations of (1) to test all the above analytical results. In our simulations, we divide a rectangular region into two parts like Fig. 2. In Fig. 3(a), a pattern of positive refraction of nonlinear waves is illustrated clearly with direct numerical simulation of Eq.(1). In Fig. 3(b), we plot the relation of incident and refractory angles in $\theta_1 - \theta_2$ plane. The circles are numerical data and the solid line is theoretical prediction, which perfectly coincide with each other, fully confirming the assumption of Eq.(4) and the prediction of (6).

Now we demonstrate negative refraction problem by simulation. In Fig.3(c) and 3(d), we take parameter combinations at which the incident waves are NWs while the refractory waves are AWs. Fig. 3(c) shows the pattern of negative refraction analogous to the novel negative refraction in linear optics [2]. Unlike the optical case, here the negative refraction is observed with nonlinear waves. In Fig. 3(d), we perform the same computation as Fig.

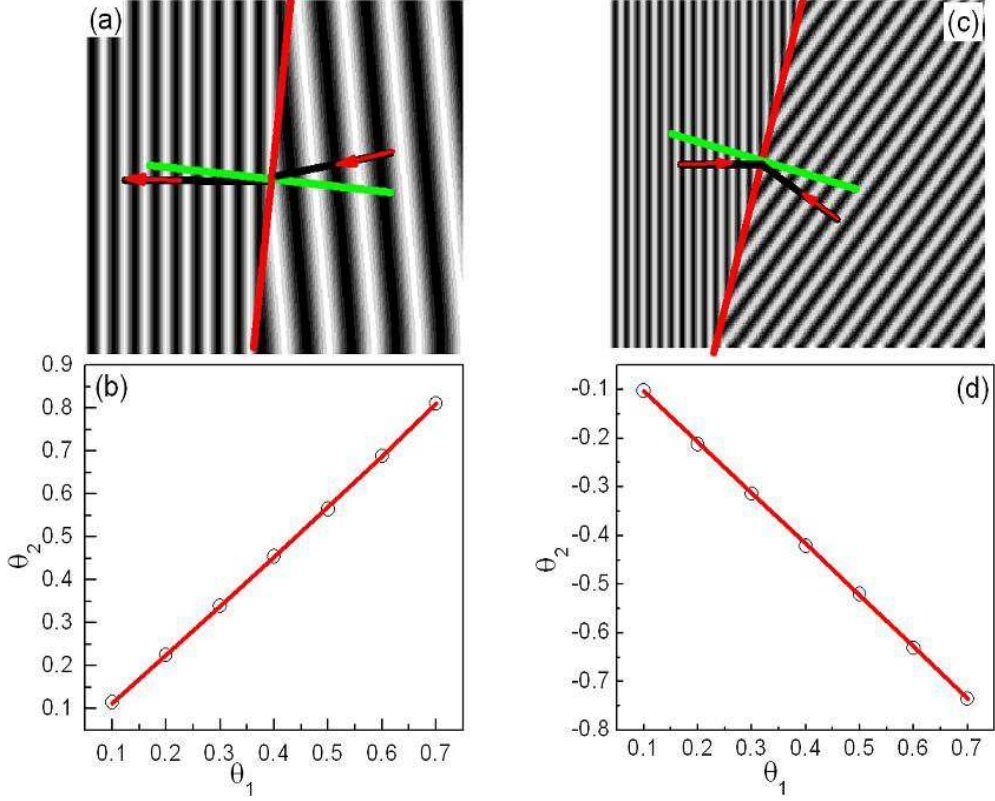


FIG. 3: (a & b) Positive refraction. (a): $\omega_{in} = 0.2$, $\theta_1 = 0.1$. Pattern of positive refraction with $\alpha_1 = 0.5$, $\beta_1 = 0.0$ (AW medium) and $\alpha_2 = 0.5$, $\beta_2 = -1.8$ (AW medium). The red line is the interface of two media. The blue line is the normal line perpendicular to the interface. The other two lines marked with arrows are the incident and the refractory lines, respectively. The arrows denote the directions of phase velocities. (b): The relation between the incident angle (θ_1) and the refractory angle (θ_2). $\alpha_1 = 0.5$, $\beta_1 = -1.0$, $\alpha_2 = 0.5$, $\beta_2 = -1.4$, and $\omega_{in} = -0.02$. Circles represent numerical results and the solid line shows theoretical predictions of Eq.(6). Both results coincide with each other perfectly. (c)&(d) $\omega_{in} = 0.02$. Negative refraction with $\alpha_1 = -0.5$, $\beta_1 = 1.4$ (NW medium) and $\alpha_2 = 0.5$, $\beta_2 = -1.4$ (AW medium). (c): Pattern of negative refraction with $\theta_1 = 0.5$. (d): The same as (b) with negative refraction considered.

3(b) by considering negative refraction, and numerical results are in perfect agreement with the theoretical predictions for negative refraction.

Since CGLE appears universally in nonlinear extended systems around Hopf bifurcation from homogenous stationary states to homogeneous oscillations, the negative refraction phenomenon found in CGLE is expected to be observed experimentally in wide range of

practical nonlinear and nonequilibrium systems. Chemical reaction diffusion (RD) systems are the most probable candidates of this kind. Here we take a well known chemical reaction model, the 2D Brusselator, as our example [18, 19]

$$\begin{aligned}\frac{\partial u}{\partial t} &= a - (b + 1)u + u^2v + \nabla^2 u + \delta(x)F \cos(\omega_R t) \\ \frac{\partial v}{\partial t} &= bu - u^2v + D\nabla^2 u\end{aligned}\tag{7}$$

In these equations, a and b are two constant chemical components, and u and v chemical variable components. All a , b , u and v are positive definite (physical constraint). Without periodic forcing, this system undergoes Hopf bifurcation to homogeneous oscillation at the parameters $b = 1 + a^2$. At the Hopf instability, the frequency of the oscillation reads $\omega_H = a$. We simulate Eq.(7) with a parameter set slightly beyond Hopf bifurcation, and find positive refraction phenomenon shown in Fig. 4(a). In Fig.4(b), we use $\omega_R = 1.05$ and parameter sets of $a = 1.0$, $D = 0.5$ and $a = 1.2$, $D = 2.25$ for the two chemical media on either side of the interface, respectively. The chemical parameter set can be transformed to CGLE parameter set by $\alpha = a\frac{D-1}{D+1}$, $\beta = \frac{7a^2-4-4a^4}{3a(2+a^2)}$ and $\omega_{in} = \frac{\omega_R-a}{\sqrt{\epsilon}}$, $\epsilon = b - (1 + a^2)$ [18]. From this correspondence, we justify NW and AW for the left and right media of Fig.4(b), respectively, and expect to observe negative refraction. Indeed, we do reveal this interesting phenomenon in the simulation of this nonlinear RD system in Fig.4(b).

In conclusion, we have generated antiwaves in CGLE and reaction diffusion systems by local periodic forcing. At fixed parameters, we can freely produce normal or anti waves by adjusting the input frequency ω_{in} . A frequency dependent refraction index $n(\omega)$ is defined for CGLE, which takes positive and negative values for NW and AW, respectively. When waves propagate from positive to negative $n(\omega)$ or vice versa, novel negative refraction emerges. The negative refraction phenomenon predicted in linear optics depends on the existence of left-handed materials which have not yet found so far in nature. In our case, nonlinear negative refraction can be observed in wide range of natural oscillatory media under suitable physical condition, i.e., Hopf bifurcation and resonance conditions. Since the complex Ginzburg-Landau equation and nonlinear waves are common in nature, we predict that the negative refraction phenomenon explored in this letter can be widely observed, and

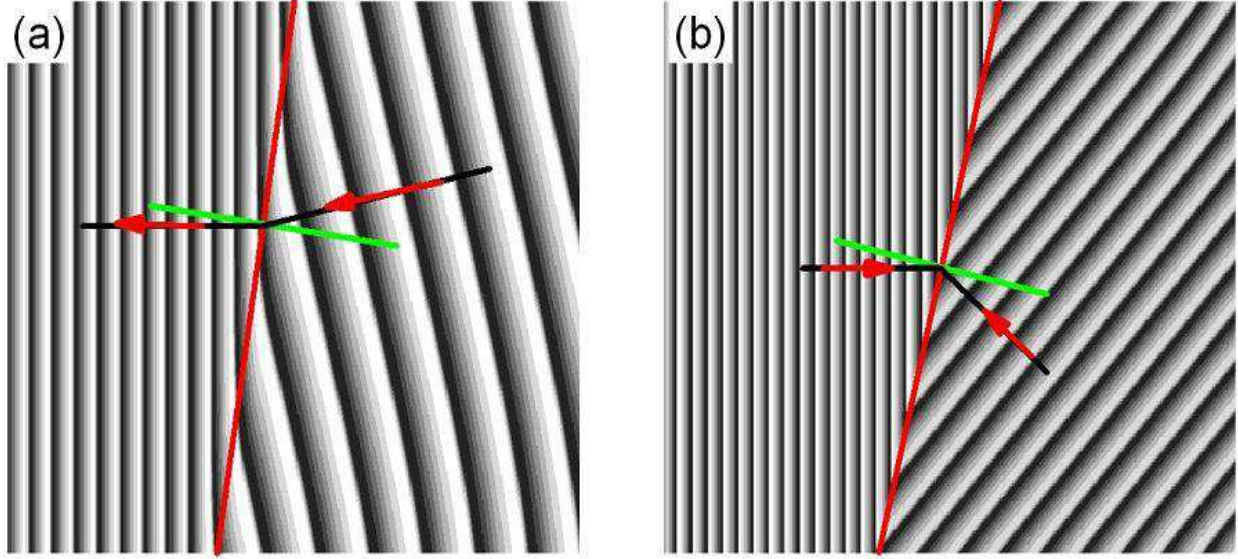


FIG. 4: Numerical simulation of Eq. (7), the periodically forced Brusselator. Time step $\Delta t = 0.01$. 400×300 physical space is discretized with 400×300 pixels and the forcing is applied on the sites of the left line of the rectangular space. $b = 3.2$. (a) Positive refraction observed between two AW media. $a = 1.2$, $D = 1.7$ for the left medium and $a = 1.2$, $D = 2.5$ for the right one. $\omega_R = 1.07$, $\theta_1 = 0.2$. (b) Negative refraction observed between NW (left) and AW (right) media. $a = 1.0$, $D = 0.5$ for the left medium and $a = 1.2$, $D = 2.25$ for the right one. $\omega_R = 1.05$, $\theta_1 = 0.3$.

that it can be realized in experiments, such as in chemical reaction experiments.

-
- [1] V. G. Veselago, *Sov. Phys. Usp.* **10**, 509 (1968); J. B. Pendry, *Phys. Rev. Lett.* **85**, 3966 (2000).
 - [2] R. A. Shelby, D. R. Smith, and S. Schultz, *Science* **292**, 77 (2001).
 - [3] V. K. Vanag and I. R. Epstein, *Science* **294**, 835 (2001).
 - [4] V. K. Vanag and I. R. Epstein, *Phys. Rev. Lett.* **87**, 228301 (2001); *Phys. Rev. Lett.* **88**, 088303 (2002).
 - [5] L. Yang, M. Dolnik, A. M. Zhabotinsky, and I. R. Epstein, *J. Chem. Phys.* **117**, 7259 (2002).
 - [6] Y. Gong and D. J. Christin, *Phys. Rev. Lett.* **90**, 088302 (2003); *Phys. Lett. A* **331**, 209 (2004).
 - [7] L. Bruschi, E. M. Nicola, and M. Bär, *Phys. Rev. Lett.* **92**, 089801 (2004); E. M. Nicola, L. Bruschi, and M. Bär, *J. Phys. Chem. B* **108**, 14733 (2004).
 - [8] P. Kim, T. Ko, H. Jeong, and H. Moon, *Phys. Rev. E* **70**, R065201 (2004).

- [9] H. Zhang, B. Hu, G. Hu, Q. Ouyang, and J. Kurths, *Phys. Rev. E* **66** 046303 (2002); H. Zhang, B. Hu, and G. Hu, *Phys. Rev. E* **68**, 026134 (2003); H. Zhang, Z. Cao, N. Wu, H. Ying and G. Hu, *Phys. Rev. Lett.* **94**, 188301 (2005).
- [10] P. Kolodner, S. Slimani, N. Aubry, and R. Lima, *Physica D* **85**, 165 (1995).
- [11] P. Coullet, L. Gil, and F. Roca, *Opt. Commun.* **73**, 403 (1989); M. S. Miguel, *Phys. Rev. Lett.* **75**, 425 (1995).
- [12] Y. Kuramoto and T. Tsuzuki, *Prog. Theor. Phys.* **52**, 536 (1974); Y. Hiramoto and S. Koga, *Prog. Theor. Phys. Suppl.* **66**, 1081 (1981).
- [13] T. Leweke and M. Provansal, *Phys. Rev. Lett.* **72**, 3174 (1994).
- [14] R. Schielen , A. Doelman, and H. de Swart, *J. Fluid Mech.* **252**, 325 (1993).
- [15] P. C. F. van der Vaart and H. K. Dijkstra, *Phys. Fluids* **9**, 615 (1993).
- [16] I. S. Aranson, and L. Kramer, *Rev. Mod. Phys* **74**, 99 (2002).
- [17] K. Mam, E. Ott, M. Gabbsy, P. N. Guzdar, *Physica D* **118**, 69 (1998).
- [18] E. M. Nicola, Bruschi L., and M. Bär, *J. Phys. Chem. B* **108**, 14733 (2004).
- [19] G. Nicolis and I. Prigogine, *Self-organization in non-equilibrium systems*, John Wiley & Sons, Inc. (1977).